Crystalline Phases in Nylon-11: Studies Using HTWAXS and HTFTIR

Smitha S. Nair and C. Ramesh*

Division of Polymer Science and Engineering, National Chemical Laboratory, Pune 411 008, India

K. Tashiro

Department of Future Industry-Oriented Basic Science and Materials, Graduate School of Engineering, Toyota Technological Institute, Nagoya 468-8511, Japan

Received December 5, 2005; Revised Manuscript Received March 6, 2006

ABSTRACT: Nylon-11 was crystallized into different crystalline phases by appropriate methods. The change in the structure during heating was monitored in situ by wide-angle X-ray scattering (WAXS). The α phase obtained by precipitating nylon-11 in 1,4-butanediol started transforming into the pseudohexagonal phase on heating, but the transformation was not fully completed before melting. The melt crystallized sample at 175 °C gave the pseudohexagonal phase, which transformed into the α′ phase on cooling to room temperature at about 100 °C. The *d* spacing of the 001 reflection also showed a change at the transition temperature. The melt-quenched sample showed the pseudohexagonal phase, which did not change during heating, but on cooling transformed into α′ phase. The γ phase was obtained by casting nylon-11 in trifluoroacetic acid (TFA), and it changed into the pseudohexagonal phase at about 110 °C on heating. The *d* spacing of the 001 reflection depended on the way in which it was obtained. The studies have shown that nylon-11 is one of the few nylons that exhibit an extensive degree of polymorphism. High-temperature Fourier transform infrared spectroscopy (HTFTIR) studies revealed, apart from the conformational differences between various phases of nylon-11, some information on the formation of the γ phase.

Introduction

Nylons are important semicrystalline polymers with many useful properties. Among nylons, nylon-6,6 and nylon-6 are commercially successful and have been extensively explored scientifically, while other nylons have received less attention. In the odd-nylons group, nylon-11 received considerable scientific attention because of its piezoelectric and ferroelectric properties. The piezoelectric and ferroelectric properties of nylon-11 have been studied in recent years[1−6] and are thought to originate from the polar structure such as in that of the α phase of odd nylon. Nylon-11 exhibits polymorphism, and several researchers[3,7−13] have studied the polymorphism of nylon-11.

The crystal structure of nylons is dominated by hydrogen bonds; hydrogen-bonded sheets are the main feature of nylon structure, and the two strong reflections arise from this feature. The *d* spacings of these reflections at 0.37 and 0.44 nm are due to the intersheet distance between the sheets and the projected interchain distance within the sheet, respectively. The important feature of nylons is that the structure undergoes a crystalline transition when subjected to heating. The crystalline transition in nylon-6,6 has been well documented and is known as the Brill transition.[14] In nylon-6,6, the room temperature α phase transforms into a pseudohexagonal structure on heating. Crystalline transition is also reported for nylons -4,6,[15] -6,10,[15] and -6,12.[15,16] Murthy et al.[17] have observed that the room-temperature monoclinic structure of nylon-6 transforms into a high-temperature monoclinic structure on heating from room temperature and considered it as the Brill transition. The changes observed in the infrared spectra of nylons -6 and -6,6 during heating have been correlated to the Brill transition.[17] Nylon-12 crystallizes[18] into the α phase on crystallization from the melt and transforms into the γ phase on subsequent cooling to room temperature.

Murthy et al.[19] suggested enhanced mobility of chains in the crystalline phase during transformation from one crystalline phase to another. Tashiro and co-workers[20−24] studied the crystalline transitions in nylons by using HTFTIR and HT-WAXS techniques in combination with the computer simulation method. Furthermore, they have used model compounds to understand the crystalline transition behavior in nylons. In the Brill transition region, the methylene segments are conformationally disordered with an invasion of gauche bonds, and the effective lengths of trans-zigzag methylene parts become shorter. This information was obtained on the basis of systematic assignments of the infrared spectra observed for a series of nylons and their model compounds. The triclinic packing structure is kept in average, but it approaches gradually to the pseudohexagonal packing mode, as proved by the molecular dynamics calculations.

Nylon-11 exhibits five crystalline modifications, including the α phase, resulting from annealing of the quenched polymer[7−9] or solution casting from *m*-cresol,[10] the α′ phase obtained from melt crystallization,[10] the pseudohexagonal phase obtained above room temperature by heating the α′ phase,[11] smectic, or δ′ phase obtained by melt quenching,[12] and the γ phase obtained by solution casting from TFA.[13] Zhang et al. have studied the crystal form transitions of nylon-11 at different drawing temperatures with different drawing ratios.[25] The crystal structure of the α phase obtained by casting from *m*-cresol and lamellar crystals grown from glycerine[9] is triclinic,[8] the amide groups lie in a plane tilted to the chain axis, and the structure is similar to nylon-6,6.[26] In the α phase of nylon-6,6, the hydrogen bonds are formed between the parallel chains. A

* Corresponding author. E-mail: c.ramesh@ncl.res.in.

10.1021/ma052597e CCC: $33.50
Published on Web 03/23/2006

monoclinic cell similar to that of nylon-6 is also suggested[10] for nylon-11 grown from the solution in water containing 5% formic acid at 160 °C. In the monoclinic structure of nylon-6, the hydrogen bonds are formed between antiparallel chains. These authors also observed another form similar to the γ phase of nylon-6.

Variable temperature wide-angle X-ray scattering is perhaps one of the most appropriate tools to study the crystalline phases and their transitions. In the present paper, we report the results of the detailed study made on the polymorphism of nylon-11. For the first time, we prepared the various crystalline forms of nylon-11 by different procedures and followed the crystalline transitions in situ by using a hot stage attached to an X-ray diffractometer. Furthermore, for the first time, we observed, in the case of nylon-11, the distinct changes in the *d* spacing of the 001 reflection during crystalline transition in the case of certain phases. Also, for the first time, we examined the FTIR spectra of various phases at room temperature and on heating and correlated it with the HTWAXS data.

Experimental Section

Nylon-11 pellets were obtained from Aldrich, USA. Nylon-11 was crystallized in the α phase by dissolving nylon-11 pellets in 1,4-butanediol at its refluxing temperature. On cooling very gradually to room temperature, the nylon-11 formed a precipitate, which was filtered and washed repeatedly in acetone to remove the 1,4-butanediol. This procedure gave a highly crystalline α phase in the form of fine powder. This powder was used for WAXS studies on the α phase of nylon-11. Room-temperature WAXS pattern showed that the sample crystallized fully into the α phase, and the crystallinity obtained by profile fitting of the peaks was 57%.

The XRD experiments were performed using a Rigaku Dmax 2500 diffractometer with a copper target. The details are described elsewhere.[27] The sample holder was a copper block, and the nylon-11 powder in the α phase was pressed on the block. The diffraction pattern was collected while the sample temperature was held constant. The change in the diffraction pattern was monitored during heating by scanning at regular temperature intervals until the sample melted. To avoid degradation, the sample was kept under vacuum during experiment. The positions of the peaks were fixed by deconvoluting the peaks by profile fitting, using Rigaku multipeak separation software available with the diffractometer system.

For melt crystallization studies, a thin film of nylon-11 was formed on the copper block by melt pressing the sample. The sample was heated well above the melting temperature (T_m) and then cooled to 175 °C, the crystallization temperature (T_c). The development of crystalline structure during the isothermal crystallization process was studied by scanning at regular time intervals. After the crystallization was completed, the sample was cooled to room temperature and scanned at different temperatures during cooling, and the change in crystal structure was monitored. The sample was again heated to melting, and the data were acquired at regular temperature intervals. In another experiment, a thin nylon-11 melt was formed on the copper sample holder and quenched in ice. During this procedure, it was made sure that ice or water was not allowed to get in contact with the nylon-11 sample. The melt-quenched nylon-11 sample was loaded in the X-ray hot stage and heated to melting, and the diffraction patterns were acquired at regular temperature intervals. In a few cases, instead of heating to melt, the heating was stopped at a certain temperature and then cooled back to room temperature.

Nylon-11 film was also cast from TFA. The film was stuck in the copper sample holder and heated to melting, and the diffraction patterns were acquired at regular temperature intervals. In one experiment, the heating was stopped at 150 °C and the sample was cooled back to room temperature.

Room temperature and high-temperature infrared spectra of these samples were taken using a Perkin-Elmer FTIR spectrometer (model Spectrum GX) with a DTGS detector at a resolution of 2 cm^{-1} in the range of 400−4500 cm^{-1}. A total of 32 scans were used for signal averaging. The high-temperature spectra were obtained by mounting the sample in a Mettler Toledo FP82HT hot stage and placing it in the sample compartment of the FTIR. The sample, in the form of powder, was sandwiched in the KBr pellet. The sample was heated at the rate of 5 °C/min. The spectra were collected while the sample temperature was held constant. The change in spectra was monitored during heating by scanning at regular temperature intervals until the sample melted. The selected regions of the spectra were profile fitted by using the Peakfit (Jandell) profile fitting program, and the profiles were assumed to be Gaussian. In the case of TFA-cast film, the film was initially heated to 120 °C to remove the residual TFA solvent from the film and then cooled to RT before starting the experiment.

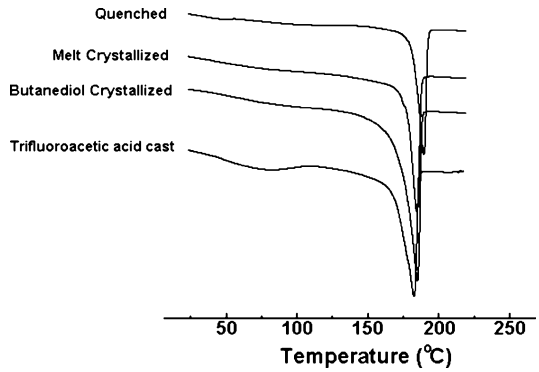

Figure 1. DSC thermograms obtained during the first heating for 1,4-butanediol crystallized, melt crystallized, quenched, and TFA-cast nylon-11.

The melting behavior of the various samples was analyzed by using a TA Instruments Q10 calorimeter. The sample weight was about 5 mg, and the heating rate was 10 °C/min. The calorimeter was calibrated using the standard protocol. The samples were scanned from 0 to 250 °C.

Results and Discussion

The calorimetric data on the nylon-11 samples will be presented first. Figure 1 shows the thermograms obtained during the first heating of nylon-11 samples crystallized by various techniques. The melt crystallized, and 1,4-butanediol crystallized samples show melting temperature at 184 °C. The sample cast from TFA has a lower melting point at 181 °C. Apart from the melting endotherm, the 1,4-butanediol-crystallized sample and the TFA-cast film show a broad endotherm at about 100 °C arising from the solvent retained in the samples even after drying in the vacuum oven at 30 °C overnight. TGA studies on the TFA-cast film showed the presence of about 5% solvent in the film. The melt-quenched sample does not exhibit crystallization exotherm, indicating that the sample crystallized despite rapid quenching. Interestingly, the quenched sample shows a higher melting temperature than that of the other samples and melts at 189 °C. In general, these thermograms do not exhibit any thermal event before melting.

The room-temperature diffraction pattern of the nylon-11 sample crystallized in 1,4-butanediol shows the characteristic reflections of nylons at $2\theta = 19.92$ and 23.74°. The corresponding *d* spacings are 0.445 and 0.374 nm, respectively. These reflections may be indexed as 100 and 110/010 based on the α phase having a triclinic unit cell proposed by Slichter,[7] Kawaguchi et al.,[9] and Kim et al.[10] The *d* spacings 0.445 and 0.374 nm correlate to the projected interchain distance within the sheet and the intersheet distance between the sheets, respectively. The 001 reflection occurs at $2\theta = 7.54°$, corresponding to a *d* spacing of 1.171 nm. The α phase may also be obtained by treating

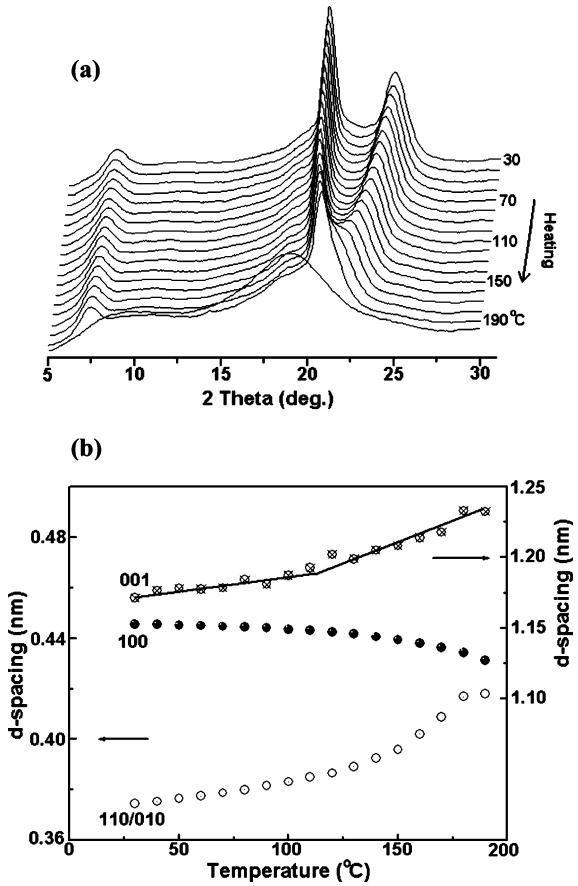

Figure 2. Behavior of (a) XRD patterns and (b) *d* spacings on heating from room temperature to melt for the α phase of nylon-11 crystallized in 1,4-butanediol.

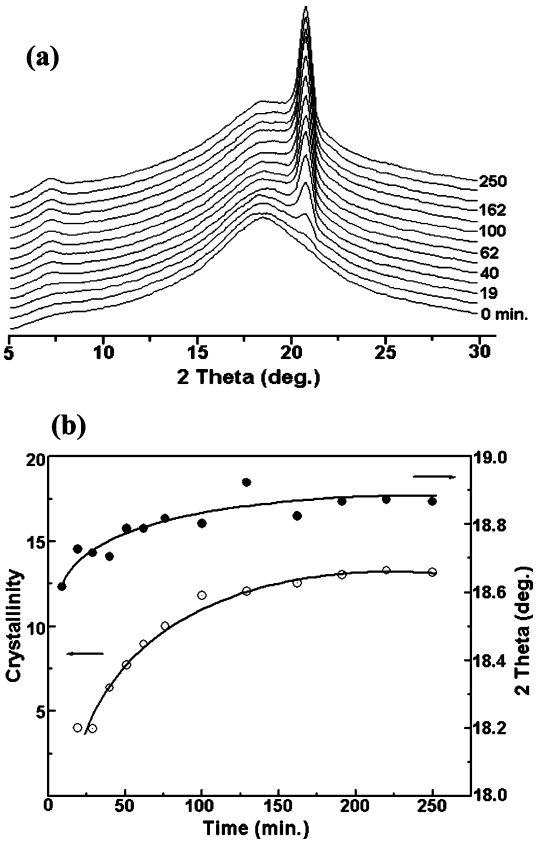

Figure 3. (a) Isothermal crystallization behavior for nylon-11 at 175 °C. (b) Degree of crystallinity and the variation of amorphous peak position during isothermal crystallization at 175 °C.

nylon-11 in glycerine at 160 °C[9] or by casting from *m*-cresol.[10] The behavior of the diffractograms and the *d* spacings of the α phase on heating from room temperature to melt is shown in Figure 2a and b, respectively. It is seen from the Figure 2 that, on heating, the two-peak nature of the diffractogram is preserved until melting. The change in the *d* spacings of 100 and 110/010 reflections with increase in temperature is reminiscent of the behavior of *d* spacings in the even−even nylons such as nylon-6,6, nylon-6,10, and nylon-6,12. The *d* spacing of the 110/010 reflection shows a rapid increase after 110 °C and approaches the 100 reflection, indicating the transformation of the α phase into the pseudohexagonal phase. However, the transformation is not fully completed before melting. Indeed, Tashiro and co-workers[20−24] have shown that the Brill transition does not occur at only one temperature point but it occurs over a temperature region. Another notable feature of the nylon-11 α phase is the behavior of the 001 peak on heating, as shown in Figure 2b. The *d* spacing of the 001 reflection increases with increase in temperature; the increase is more rapid at about 110 °C, similar to the *d* spacing of 110/010 reflections. In general, with an increase in temperature, a small decrease in the 001 reflection *d* spacing is expected because of the enhanced motion of the methylene segments.[20,21] The higher mobility of the methylene segments is a general feature of all nylons at elevated temperatures.[20,21] In the present case, the increase in the *d* spacing of the 001 reflection with an increase in temperature may be attributed to the decrease in the angle made by the normal of the 001 plane to the *c* axis. The variations in diffraction patterns and *d* spacings on heating from room temperature are found to be reversible if the sample is not allowed to melt, but held at temperatures below the T_m and then cooled to room temperature.

The behavior of the diffractograms and *d* spacings of the melt-crystallized sample is different from the sample crystallized from the 1,4-butanediol solution described above. The diffraction patterns obtained during isothermal melt crystallization of nylon-11 at 175 °C are shown in Figure 3a. The initially amorphous sample slowly crystallizes, and the diffraction pattern shows the development of crystalline peaks at $2\theta = 6.93°$ and 20.69° with an increase in time. The corresponding *d* spacings are 1.274 and 0.429 nm. The reflection at $2\theta = 6.93°$ arises from the chain repeat unit and may be indexed to the 001 reflection. The *d* spacing value, 1.274 nm, which is much lower than the extended chain length of 1.5 nm, indicates that, in the melt crystallization also, the normal of the 001 plane is tilted with respect to the *c* axis. Hence, the single single peak at $2\theta = 20.69°$ indicates that the sample crystallized in the pseudo-hexagonal phase-like nylon-6,6[14,28] at 175 °C.

During isothermal crystallization, the degree of crystallinity increases with an increase in crystallization time, and after about 3 h, it remains almost constant even with a further increase in crystallization time, as shown in Figure 3b. The figure also shows the shift in the amorphous peak position to higher angles with an increase in crystallization time. This indicates the densification of the amorphous region with an increase in crystallinity. Hence, caution should be exercised when assuming amorphous phase density for the quantitative determination of crystallinity using density techniques.

The behavior of the diffractograms and the *d* spacings on cooling from T_c to room temperature is shown in Figure 4a and b, respectively. It is seen from the Figure 4a that, on cooling from the crystallization temperature, the single-peak nature of

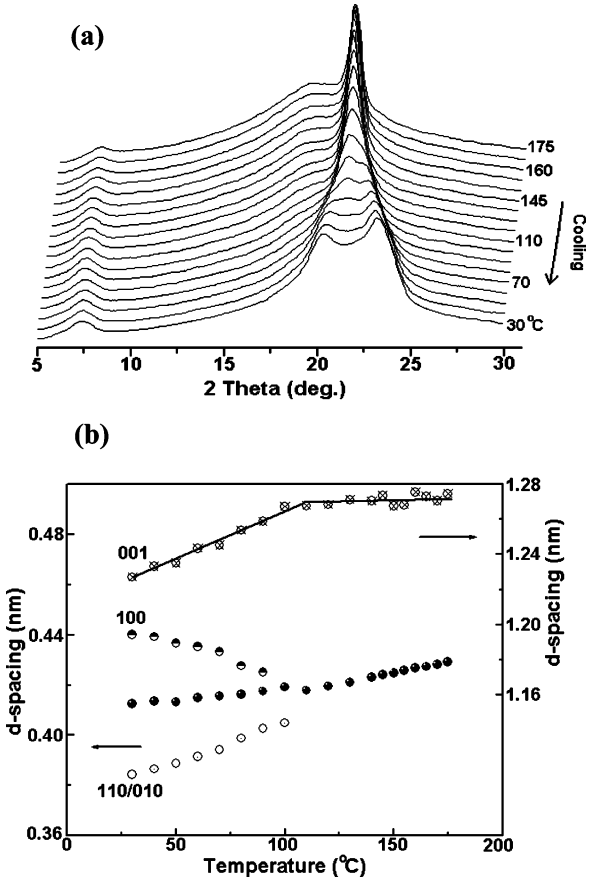

Figure 4. Behavior of (a) XRD patterns and (b) *d* spacings of nylon-11 melt crystallized at 175 °C on cooling to room temperature.

the diffractogram is preserved and the *d* spacings of the pseudohexagonal phase show small decreases with further decrease in temperature. However, two new peaks at $2\theta = 20.89°$ and 21.94° appear at about 100 °C. These peaks become prominent and separate out with further decrease in temperature, and concomitantly, the peak due to the pseudohexagonal phase decreases. This indicates a crystalline transition of the pseudohexagonal phase at about 100 °C. At room temperature, these new peaks appear at $2\theta = 20.17°$ and 23.13°, and the corresponding *d* spacings are 0.440 and 0.384 nm. The 001 reflection now occurs at $2\theta = 7.20°$, and the corresponding *d* spacing is 1.227 nm. These *d* spacings at room temperature are different from the *d* spacings of the α phase discussed above. Furthermore, the behavior of the diffractograms with temperature is different from that of the α phase. Hence, we designate this phase as the α′ phase[10] to distinguish it from the α phase obtained by crystallizing in 1,4- butanediol. The pseudohexagonal phase peak is not obvious in the diffraction pattern below 70 °C; however, the profile fitting of the peaks clearly shows the presence of the pseudohexagonal phase peak even at room temperature. At room temperature, the pseudohexagonal phase fraction is about 4% and that of the α′ phase is about 46%. In the temperature range 30−100 °C, the peak at $2\theta = 6.93°$ is attributed only to the α′ phase because the amount of the pseudohexagonal phase is too low to identify the position of the 001 reflection. The peak at $2\theta = 6.93°$, which is due to the 001 reflection, shows interesting behavior and is shown in Figure 4b. The *d* spacing of this reflection remains constant in the pseudohexagonal phase, but starts to decrease after its transformation to the α′ phase at 100 °C. The variations in diffraction patterns and *d* spacings on cooling from T_c are found to be reversible on heating the sample from room temperature to melting. However, a small

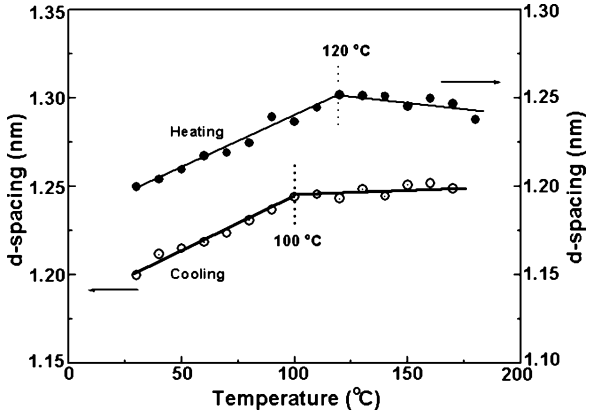

Figure 5. Behavior of the *d* spacings of the 001 reflection on cooling from T_c to room temperature and on heating from room temperature to melting.

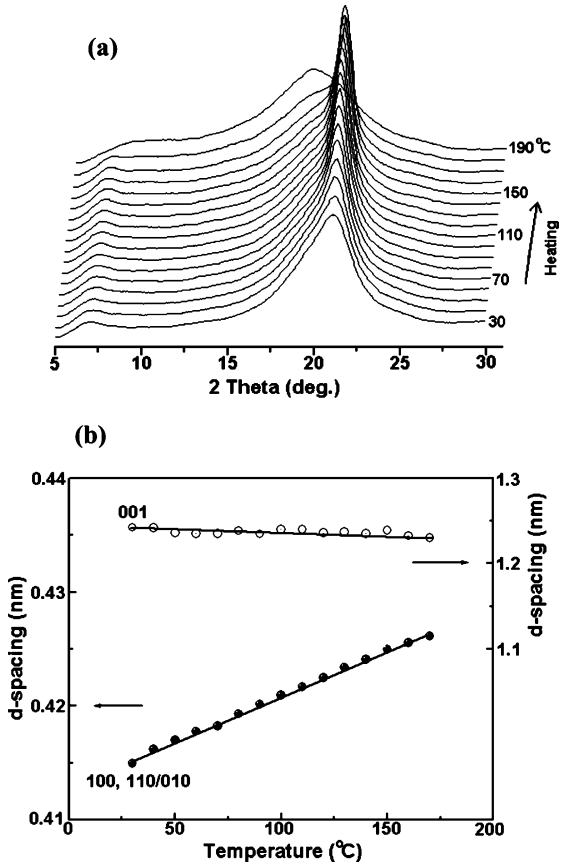

Figure 6. Behavior of (a) XRD patterns and (b) *d* spacings on heating from room temperature to melt for quenched nylon-11.

shift in the transition temperature is noted between the cooling and heating cycle and is more clearly seen in the plot of the *d* spacing of the 001 reflection, shown in Figure 5. The transition temperature occurs at 100 °C on cooling and at 120 °C on heating. Such a hysteresis in the transition temperature is shown for nylon-6,6 and is indicative of first-order transition.[28]

Another phase reported for nylon-11 is the smectic phase or the δ′ phase and is obtained by rapidly quenching the melt. Parts a and b of Figure 6 show diffractograms and *d* spacings of the melt-quenched sample on heating from room temperature. The room-temperature diffractogram looks very broad, similar to the amorphous material, but the definite peak at $2\theta = 7.11°$ arising from the 001 reflection shows that the material is indeed crystalline. Profile fitting the broad peak brings the crystalline peak at $2\theta = 21.43°$. On heating, the single peak at $2\theta = 21.43°$

Table 1. Crystallization/Holding Temperature (T_c) and Transition Temperature (T_B) of Nylon-11

T_c (°C)	T_B (°C)	$T_c - T_B$ (°C)
175[a]	100	75
170	100	70
150	80	70
120	70	50

[a] Melt crystallized sample. Others are melt quenched and heated to the respective temperatures. The cooling rate of the hot stage is too limiting to study the crystallization behavior of the samples below 175 °C, as the sample crystallizes very rapidly before reaching the intended crystallization temperature.

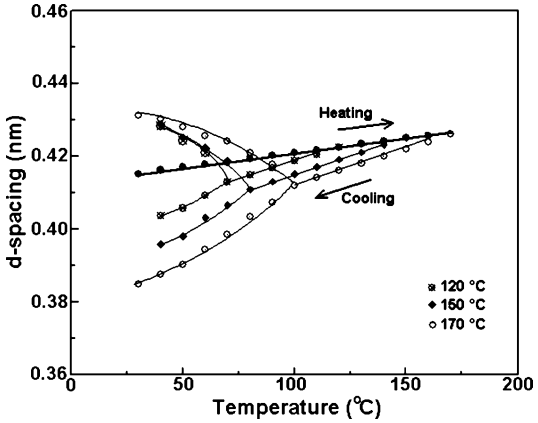

Figure 7. Behavior of the *d* spacings of the melt quenched sample on heating to 170 °C and on cooling from the holding temperatures 170, 150, and 120 °C to room temperature. The arrows indicate the direction of heating/cooling.

becomes sharper and shifts to lower angles, and the single-peak nature is preserved until melting. The position of the peak at $2\theta = 7.11°$ does not vary with heating. These results indicate that the δ' phase progressively transforms into the pseudohexagonal phase, as discussed earlier in the text. Alternatively, it may be thought of that the smectic phase or the δ' phase is indeed the pseudohexagonal phase with highly defective crystals, and on heating, these crystals become more perfect. A similar behavior also is exhibited by rapidly quenched nylon-6,6.[29]

The behavior of the sample is different, however, if it is not allowed to melt but held at temperatures below the T_m and then cooled to room temperature. The diffractograms obtained on cooling from the holding temperature 170 °C show that the pseudohexagonal structure transformed into the α' phase by the appearance of its characteristic peaks at about 100 °C. However, in this sample, the pseudohexagonal phase is not very obvious below 100 °C, as in the case of the melt-crystallized sample at 175 °C, and hence, it is not considered during the profile-fitting procedure. A similar behavior is observed for holding temperatures 150 and 120 °C; however, the transition temperature shifts to lower temperatures. For holding temperatures below 100 °C, the peaks could not reliably be separated; the peaks show broadening on cooling. Table 1 shows the holding temperatures and the corresponding transition temperatures (T_B). Another important point to be noted is that, on cooling from 170 to 100 °C, the characteristic *d* spacing of the pseudohexagonal phase does not retrace the *d* spacing obtained on heating, as shown in Figure 7. Instead, the *d* spacings on cooling depend on the holding/crystallization temperature, and such a behavior is different from the behavior of nylons -6,6[28] and -6,10.[15] Furthermore, the observed difference in the *d* spacings of the pseudohexagonal phase at a given temperature depending on whether the temperature is approached on heating the quenched sample or on cooling from the holding temperatures, indicates

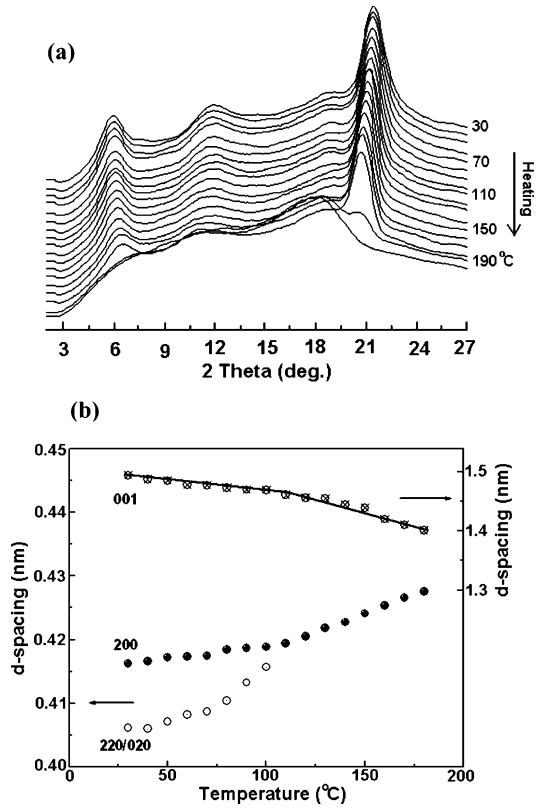

Figure 8. Behavior of (a) XRD patterns and (b) *d* spacings on heating from room temperature to melt for γ phase obtained by casting nylon-11 film from TFA. The indexing is based on the *c* axis along the chain direction.

that there exists a subtle difference in the pseudohexagonal phase during heating and cooling.

The nylon-11 cast from TFA exhibits the γ phase and appears similar to the γ phase of nylon-6 obtained by treating in KI/I_2 solution, and the room-temperature diffraction pattern can be seen in Figure 8a. The γ phase may also be obtained by exposing a melt-crystallized sample in 10% sodium hydroxide solution.[30] Though at room temperature the diffractogram appears to have a single peak at $2\theta = 21.34°$, the profile-fitting procedure clearly indicates the presence of a shoulder at $2\theta = 21.87°$. The corresponding *d* spacings of these reflections are 0.416 and 0.406 nm, respectively. The peak due to the 001 reflection is seen at $2\theta = 5.91°$, and the *d* spacing is 1.495 nm. Because the fully extended repeat unit of nylon-11 is 1.5 nm, in the γ phase, the chain axis coincides with the *c*-axis of the unit cell. Although the detailed structure of the γ phase is not available in the literature, it can be thought of as monoclinic, but it is different from the monoclinic structure of form II discussed by Kawaguchi et al.[9] The changes in the diffraction pattern and the *d* spacings during heating from room temperature to melting are shown in Figure 8a and b. On heating, the peak at $2\theta = 21.87°$ moves closer to the peak at $2\theta = 21.34°$ and merges into a single peak at about 110 °C. On further heating, the single peak remains as a single peak until melting. Concomitantly the 001 reflection shows a small decrease in its *d* spacing. These data indicate that the γ phase transforms into a pseudohexagonal phase at 110 °C, which is distinctly different from the pseudohexagonal phase discussed earlier based on the 001 *d* spacings.

It is evident from the Figure 8 that the γ phase transforms into the pseudohexagonal phase at about 110 °C on heating and remains in the pseudohexagonal phase until melting. Above 110 °C, the *d* spacing of the pseudohexagonal phase increases with

an increase in temperature. If the pseudohexagonal phase is not allowed to melt, but held at temperatures below the T_m and then cooled to room temperature, it transforms back into the γ phase at about 90 °C. The room-temperature diffraction pattern of the γ phase, as obtained immediately after casting from the TFA, and the diffraction pattern taken at room temperature after heating to 150 °C appear very similar, indicating that the transformation is reversible. On heating, the 001 reflection shows a minor shift to a higher angle side, indicating a decrease in the *d* spacing. The *d* spacing of the 001 reflection and the change at the γ phase to the pseudohexagonal phase transition at 110 °C is shown in Figure 8b.

The foregoing discussions indicate that nylon-11 exists in the pseudohexagonal phase at temperatures above 110 °C; however, 001 *d* spacing and its variation with temperature depends on the starting phase. It also means that the pseudohexagonal phase obtained from the different phases has a different packing mode. This is the first report on pseudohexagonal phases having different types of packing in a single nylon.

The foregoing discussions are primarily focused on the structure based on the data obtained from variable temperature WAXS studies, and in the following section, the discussion will be focused on the data obtained from variable-temperature FTIR studies on the various phases of nylon-11. WAXS is sensitive to the changes in the unit cell, while FTIR is sensitive to conformational changes. FTIR spectra of nylons are well documented in the literature[31] and have four important regions. The region 500−800 cm^{-1} comprises the amide V and VI bands. The 1000−1400 cm^{-1} region contains the so-called progression bands and is sensitive to the methylene segments. The region 1500−1700 cm^{-1} contains the amide I and II bands and is sensitive to N−H stretching and C−O bonds. The amide A band occurs at about 3300 cm^{-1} and is assigned to N−H stretching vibration and is sensitive to the strength of the hydrogen bond.

The room-temperature spectra of selected regions of α, α′, and γ phases are shown in Figure 9a−d. Most importantly, the spectra of α and α′ phases show very subtle differences; however, the γ phase spectra is distinctly different from the spectra of α and α′ phases but show close similarity to the nylon-6 γ phase. Figure 9a shows the spectral region from 400 to 800 cm^{-1} for the various phases and comprises the amide V and amide VI bands. At room temperature, the amide V and VI bands appear at 686 and 582 cm^{-1}, respectively, for the α phase (1,4-butanediol-crystallized sample). These bands appear at 686 and 581 cm^{-1} for the α′ phase (melt-crystallized sample). The amide V band shifts from 686 to 709 cm^{-1} for the γ phase (TFA-cast film). Furthermore, in the case of the γ phase, the amide VI band is shifted[29] from 582 to 627 cm^{-1}. Similar to the γ phase of nylon-6,[32] the spectra show a distinct additional band at 595 cm^{-1}, which is characteristic of the γ phase.[32]

Another region of interest is from 1100 to 1400 cm^{-1} and is characterized by the progression bands from the methylene sequence. Figure 9b shows this region, and the bands appear at 1126, 1159, 1190, 1223, 1240, 1279, and 1373 cm^{-1} for the α phase at room temperature. These bands appear essentially at the same position for the α′ phases. These bands, however, appear at a different position for the γ phase and occur at 1123, 1160, 1198, 1225, 1250, 1279, and 1371 cm^{-1}, respectively.

The regions sensitive to hydrogen bonding are from 1600 to 1800 cm^{-1} and from 3000 to 3600 cm^{-1}. The region 1600−1800 cm^{-1} is shown in Figure 9c for α, α′, and γ phases and contains the amide I and amide II bands. The amide I band appears at 1640 and 1637 cm^{-1} for α and α′ phases, respectively, while for the γ phase, it is again at 1640 cm^{-1}. Visual

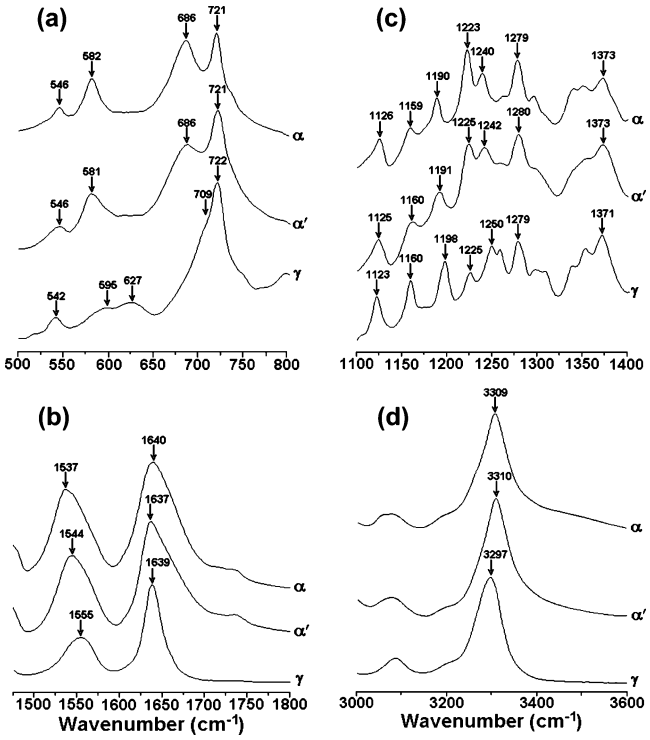

Figure 9. Room-temperature FTIR spectra of α phase (1,4-butanediol crystallized), α′ phase (melt crystallized), and γ phase (TFA cast) of the region (a) 500−800 cm^{-1}, (b) 1100−1400 cm^{-1}, (c) 1500−1800 cm^{-1}, and (d) 3000−3600 cm^{-1} of nylon-11.

inspection of Figure 9c shows that the amide I band looks very similar for α and α′ phases at room temperature. The amide I band of the γ phase, however, shows variance from the α and α′ phases; the band is considerably sharper. The amide II band appears at 1537 and 1544 cm^{-1} for α and α′ phases, respectively. The amide II band shifts to 1552 cm^{-1} for the γ phase. The amide II band arises mainly from the in-plane N−H bending and has contributions from ordered, disordered, and free N−H groups. Consequently, the amide II band also appears highly skewed.

The amide A band is assigned to N−H stretching vibration and is sensitive to the strength of the hydrogen bond and shown in Figure 9d. The contribution to the amide A comes from (i) free N−H stretch at 3444 cm^{-1}, (ii) bonded N−H stretch at 3300 cm^{-1} arising out of crystalline fraction, and (iii) bonded N−H stretch at 3310 cm^{-1} arising out of an amorphous fraction. The amide A band appears at 3309 and 3310 cm^{-1} for α and α′ phases, respectively. In the case of γ phase, it shifts to 3297 cm^{-1}. Another noticeable difference between the α and γ phases is the absorbance of the amide A band in relation with the bands at 2851 and 2920 cm^{-1}, which are assigned to symmetric and antisymmetric CH_2 stretch, respectively.[31,33] The amide A band of α and α′ phases has comparable peak height with the band at 2920 cm^{-1}, but the amide A band of the γ phase shows much reduced absorbance. The characteristic bands discussed in the preceding paragraphs show a systematic shift in wavenumbers and decrease in absorbance with increase in temperature, with subtle variation at the transition temperatures. Hence, the changes in the spectra on heating are not discussed in detail here.

The WAXS studies presented above clearly indicate that α and α′ phases are distinctly different, and on heating, the α phase does not fully transform into the pseudohexagonal phase. The α′ phase, however, transforms into the pseudohexagonal phase before melting. On the other hand, FTIR spectra show

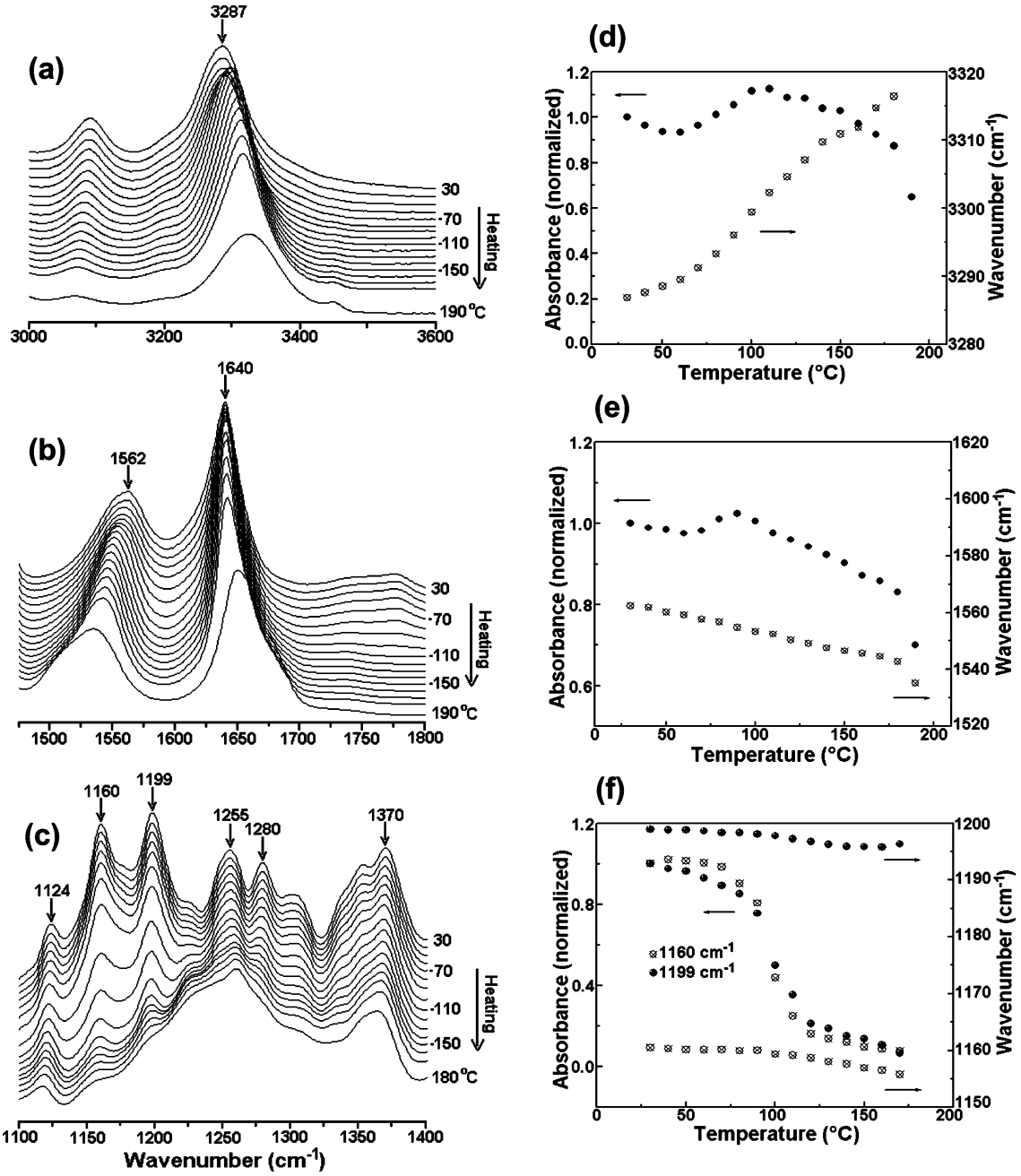

Figure 10. Variable temperature FTIR spectra of the TFA cast nylon-11 film with 5% TFA during heating from room temperature to melt: (a) 3000−3600 cm^{-1}, (b) 1500−1800 cm^{-1}, and (c) 1100−1400 cm^{-1}. The variation of the wavenumber and normalized absorbance of the characteristic bands (d) 3000−3600 cm^{-1}, (e) 1500−1800 cm^{-1}, and (f) 1100−1400 cm^{-1}.

subtle difference between these phases, indicating these two phases have similar molecular conformation in the crystalline phase. The γ phase shows distinct differences in the FTIR spectra when compared with α and α' phases. Because the conformation in the amorphous phase is expected to be the same for all the phases, the differences may be attributed to a different conformation in the γ phase.

The FTIR spectra of the γ phase of nylon-11 are similar to the spectra of the γ phase of nylon-6. In the case of nylon-6, the γ phase is obtained by KI/I_2 treatment or by melt crystallization with clay layers controlling the hydrogen bonds. In the case of the γ phase obtained by KI/I_2 treatment, the iodine forms a complex with the nylon-6, and the removal of iodine from the complex leads to the γ phase.[34] TGA studies have indicated that about 5% of the TFA is trapped in the nylon-11 film, and it leaves the sample between 70 and 110 °C on heating. It is expected that the residual solvent remains in the amorphous phase and, hence, is insensitive to the X-ray diffraction data discussed in the earlier section. Parts a−c of Figure 10 shows the FTIR spectra obtained from the cast film with 5% TFA. The spectra show variation in the amide A, amide II, and progression bands during heating. The normalized absorbance of the amide A and amide II bands shown in Figure 10d and e increases in the temperature range from 70 to 110 °C and then decreases on further heating. The progression bands at 1160 and 1199 cm^{-1}, arising from T_{10} and T_9 (CH_2 twisting) modes, also show the effect of TFA, as shown in Figure 10c and f. The wavenumber decreases with increasing temperature, but distinctly shows deviation at about 90 °C. More significantly, the absorbance of these peaks decrease very rapidly at about 90 °C when the TFA leaves the sample. The rapid decrease in the absorbance indicates the constraint in the twisting motion

of CH_2. In the case of the nylon-11−TFA system, in the solution, the amide group in the nylon can be protonated[35,36] and can form an ion pair with TFA. During the evaporation of the solvent, the ion pair disappears and the hydrogen bonding between nylon chains is gradually formed. The 5% TFA retained in the amorphous phase is also expected to form an ion pair with the amide group. On removal of the TFA on heating, the amide groups become free, which can subsequently form the hydrogen bond, and consequently, the intensity of the amide II and amide A absorbance increases and concomitantly the increased hydrogen bonding restricts the T_{10} and T_9 (CH_2 twisting) modes. The above results suggest that the formation of the γ phase in nylons may be by externally regulating the hydrogen bond formation during crystallization. In the case of nylon-6, the KI−nylon complex or the clay layers when nylon-6 is crystallized in the presence of clay layers control the hydrogen bonding formation. In the case of nylon-11, the TFA−amide ion pair controls the formation of hydrogen bonding leading to the γ phase.

Conclusion

The high-temperature XRD studies provided new information on the polymorphism of nylon-11. Nylon-11 may be crystallized into α, α', γ, and pseudohexagonal phases by appropriate crystallization conditions. Nylon-11 crystallized in the α phase when precipitated in 1,4-butanediol and did not fully transform into the pseudohexagonal phase on heating. A complex polymorphism has been exhibited by nylon-11 melt crystallized at 175 °C. The sample crystallized in the pseudohexagonal phase, and on cooling from the T_c, it transformed into the α' phase, which is different from the α phase, at about 100 °C. However, the transition temperature is dependent on the crystallization temperature. The smectic phase or the δ phase obtained on melt quenching appeared to be the pseudohexagonal phase. It was shown for the first time that the γ phase, obtained by casting nylon-11 in TFA, transformed into the pseudohexagonal phase on heating above 110 °C.

For the first time, we reported the observation of change in the 001 *d* spacing during phase transition. The value and the variation of the *d* spacing of the 001 reflection is highly phase sensitive. The 001 *d* spacing showed a change in the value when the α and α' phase changed into the pseudohexagonal phase or vice versa. Similar changes were seen when the γ phase transformed into the pseudohexagonal phase on heating to melt. The above studies indicate that nylon-11 showed a change in the structural features above 110 °C on heating, which manifested as a change in the crystalline phase.

The variable-temperature FTIR studies indicated that the α and α' phases had a similar conformation in the crystalline phase. The γ phase showed characteristic infrared bands at different positions from those of the α and α' phase. It was speculated from the HTFTIR studies on TFA-cast film with 5% TFA that the interaction of TFA with amide groups might be responsible for the formation of the γ phase.

Acknowledgment. We thank Dr. S. Sivaram, Director, National Chemical Laboratory, for his keen interest and encouragement during the course of this work. We also thank Dr. S. Ponrathnam, PSE Division, for useful discussions. S.S.N. acknowledges the Council of Scientific and Industrial Research, New Delhi, for the award of a research fellowship.

References and Notes

(1) Newman, B. A.; Chen, P. K.; Pae, K. D.; Scheinbeim, J. I. *J. Appl. Phys.* **1980**, *51*, 5161.
(2) Mathur, S. C.; Scheinbeim, J. I.; Newman, B. A. *J. Appl. Phys.* **1984**, *56*, 2419.
(3) Lee, J. W.; Takase, Y.; Newman, B. A.; Scheinbeim, J. I. *J. Polym Sci., Polym. Phys.* **1991**, *29*, 273.
(4) Takase, Y.; Lee, J. W.; Scheinbeim, J. I.; Newman, B. A. *Macromolecules* **1991**, *24*, 6644.
(5) Scheinbeim, J. I.; Lee, J. W.; Newman, B. A. *Macromolecules* **1992**, *25*, 3729.
(6) Gao, Q.; Scheinbeim, J. I. *Macromolecules* **2000**, *33*, 7564.
(7) Slichter, W. P. *J. Polym. Sci.* **1959**, *36*, 259.
(8) Kinoshita, Y. *Macromol. Chem.* **1959**, *33*, 1.
(9) Kawaguchi, A.; Ikawa, T.; Fujiwara, Y.; Tabuchi, M.; Konobe, K. *J. Macromol. Sci., Phys. B* **1981**, *20*, 1.
(10) Kim, K. G.; Newman, B. A.; Scheinbeim, J. I. *J. Polym. Sci., Polym. Phys. Ed.* **1985**, *23*, 2477.
(11) Newman, B. A.; Sham, T. P.; Pae, K. D. *J. Appl. Phys.* **1977**, *48*, 4092.
(12) Schmidt, G. F.; Stuart, H. A. *Z. Naturforsch., A* **1958**, *13*, 222.
(13) Sasaki, T. *J. Polym. Sci., Part B: Polym. Lett.* **1965**, *3*, 557.
(14) Brill, R. J. *J. Prakt. Chem.* **1942**, *161*, 49.
(15) Ramesh, C. *Macromolecules* **1999**, *32*, 3721.
(16) Biangardi, H. J. *J. Macromol. Sci., Phys. B* **1990**, *29*, 139.
(17) Vasanthan, N.; Murthy, N. S.; Bray, R. G. *Macromolecules* **1998**, *31*, 8433.
(18) Ramesh, C. *Macromolecules* **1999**, *32*, 5704.
(19) Murthy, N. S.; Curran, S. A.; Aharoni, S. M.; Minor, H. *Macromolecules* **1991**, *24*, 3215.
(20) Yoshioka, Y.; Tashiro, K.; Ramesh, C. *Polymer* **2003**, *44*, 6407.
(21) Yoshioka, Y.; Tashiro, K. *J. Phys. Chem. B* **2003**, *107*, 11835.
(22) Yoshioka, Y.; Tashiro, K. *Polymer* **2003**, *44*, 7007.
(23) Yoshioka, Y.; Tashiro, K. *Polymer* **2003**, *44*, 4337.
(24) Yoshioka, Y.; Tashiro, K. *Polymer* **2004**, *45*, 6349.
(25) Zhang, Q.; Mo, Z.; Zhang, H.; Liu, S.; Cheng, S. Z. D. *Polymer* **2001**, *42*, 5543.
(26) Bunn, C. W.; Garner, E. V. *Proc. R. Soc. London* **1947**, *189*, 39.
(27) Ramesh, C.; Gowd, E. B. *Macromolecules* **2001**, *34*, 3308.
(28) Ramesh, C.; Keller, A.; Eltink, S. J. E. A. *Polymer* **1994**, *35*, 2483.
(29) Sandeman, I.; Keller, A. *J. Polym Sci.* **1956**, *19*, 401.
(30) Yu, H. H. *Mater. Chem. Phys*. ***1998***, *56*, 289.
(31) Jakes, J.; Krimm, S. *Spectrochim. Acta, Part A* **1971**, *27*, 19.
(32) Nair, S. S.; Ramesh, C. *Macromolecules* **2004**, *37*, 454.
(33) Doskocilova, D.; Pivcova, H.; Schneider, B.; Cefelin, P. *Collect. Czech. Chem. Comm.* **1963**, *28*, 1867.
(34) Abu-isa, I. *J. Polym. Sci., Part A-1* **1971**, *9*, 199.
(35) Kricheldorf, H. R. *Makromol. Chem.* **2003**, *179*, 2695.
(36) Bradbury, J. H.; Yuan, H. H. H. *Biopolymers* **2004**, *11*, 661.

MA052597E